

Fullerene shape transformations via Stone-Wales bond rotations

Yufeng Zhao, Yu Lin, and Boris I. Yakobson*

Department of Mechanical Engineering and Materials Science, and Department of Chemistry, Rice University, Houston, Texas 77005, USA

(Received 23 April 2003; revised manuscript received 5 August 2003; published 12 December 2003)

Coalescence of fullerene cages and nanotubes can lead to the formation of novel and useful structures. We analyze the Stone-Wales (SW) paths for such fusion processes, compute and compare their energy costs, and demonstrate how the paths are determined by the initial orientation of the merging fragments. We also emphasize the versatility of SW transformation by presenting the topological possibility of the gradual penetration of a buckyball through the wall of a nanotube.

DOI: 10.1103/PhysRevB.68.233403

PACS number(s): 61.46.+w, 68.65.-k

Studies of fullerene isomerization¹ have recognized the key role of a particular atomic rearrangement called Stone-Wales (SW) or pyraclyene transformation, i.e., a 90° bond rotation within the plane of a sp^2 -carbon network, which were later found applicable to fullerene coalescence.²⁻⁵ This transformation has lower activation barrier compared to any other atomic relocation (interstitial or vacancy diffusion, etc.) while it permits pentagons and hexagons to gradually drift over the surface of a fullerene cage. Also, it has been recognized that random SW flips can be biased by the mechanical strain externally applied to the lattice, thus representing dislocation glide steps in terms of crystal physics.⁶ This reveals the important possibility of mechanical relaxation in carbon nanotubes, at least at high temperatures.⁷

While isomerization events¹ correspond to monomolecular reactions, $A \rightarrow A_1 \rightarrow A_2 \rightarrow \dots$, lately another group of relaxation processes has attracted a great deal of interest. These correspond to the fusion of two initially separate cages, a bimolecular process $A + B \rightarrow AB$, as observed in several cases of such “nanowelding,” usually at high temperatures or under an electron beam.⁸

Recent theoretical analyses and simulations of cap-to-cap coalescence of various nanotubes, as well as cap-to-wall welding,^{3,4} showed that SW paths could always be found, although there is no rigorous proof that this is universally the case. Interestingly, the revealed “depth” of coalescence has gradually increased, when traced through a series of studies. Primary linking has been investigated in the polymerization of C_{60} cages by several groups.^{9,10} The structure and formation of a joint hollow cage have been considered related to negative curvature.^{10,11} Ueno *et al.*² first reported a complete, “seamless” fusion of two buckyballs through a series of SW rotations, where a specific path was found through a computational search. Finding the most favorable SW path connecting two substantially different shapes can be a challenging task considering the tremendous number of possibilities, $N!/(N-n)!$, with n being the number of rotated bonds of the N total bonds in the merging cages. A computational search, even assisted by several constraints, can hardly go beyond several tens of steps for a system with 120 atoms.² Some analytical guidelines provided in Refs. 3 and 4, although could not be formalized into a rigorous algorithm, prove to be helpful in identification of the SW paths of substantial depth (up to 68 in Ref. 3 and up to 237 steps in this report, below).

Several examples provide convincing evidence of the possibility of fusion, with the main sequences of SW rotations being generally similar. In contrast, we note that the initial stage differs according to initial orientations of the merging cages. This is important in view of potential applications of such welding process when heterogeneous nanoelectronic components (T junction, rectifying segments, quantum dots, etc.¹²) can be engineered by welding of precisely oriented, separate units. Even for identical components like a pair of buckyballs, the path is determined by their initial docking, or mutual orientation before the covalent bonding occurs, as is shown below.

In this paper, we analyze the SW sequences for $C_{60} + C_{60} \rightarrow C_{120}$ coalescence, compare the corresponding nucleation barriers,¹³ and discuss transferability to the case of nanotubes. Then we present, as illustration of the surprising topological versatility of SW sequences, an extremely long process in which an exterior buckyball continuously penetrates through the perfect wall of a nanotube and enters its interior, as in a peapod arrangement.¹⁴

Due to the interest in cap-to-cap fusion of single-walled carbon nanotubes (SWNT's), we previously derived a SW sequence that transforms two (5,5)-nanotube caps into a section of continuous (5,5) tube.³ In this case the geometry of the nanotube imposes a specific orientation at the beginning of the process, an apex pentagon-to-pentagon docking, like **5)(5**. The most favorable is the $\pi/5$ -staggered [rotated around the nanotubes axes, see Fig. 1(a) in Ref. 3] initial orientation of the pentagons, **5)(5'**. This directly suggests the same SW path, **5)(5'**, for the buckyballs.⁴ In the presence of a series of C_{60} 's in a peapod, such a path is transferable, that is, it can be repeated after some short tubular segments have already formed and can eventually lead to transformation into a (5,5) tube inside the (10,10).

For a pair of free buckyballs, another initial docking has been considered,² which has two aligned double bonds, each one in the center of 5/6/6/5 pyraclyene. Denoted here correspondingly as **P)(P**, this orientation conveniently permits standard polymerization as the first step.⁹ Figure 1 shows the initial steps for both **P)(P** path² and **5)(5'** path,³ and the energies computed for the intermediate structures using both tight-binding¹⁵ and first principles¹⁶ methods. In both cases the highest energy structure is no. 2, where a purely SW sequence begins. In the **5)(5'** path, the initial orientation of

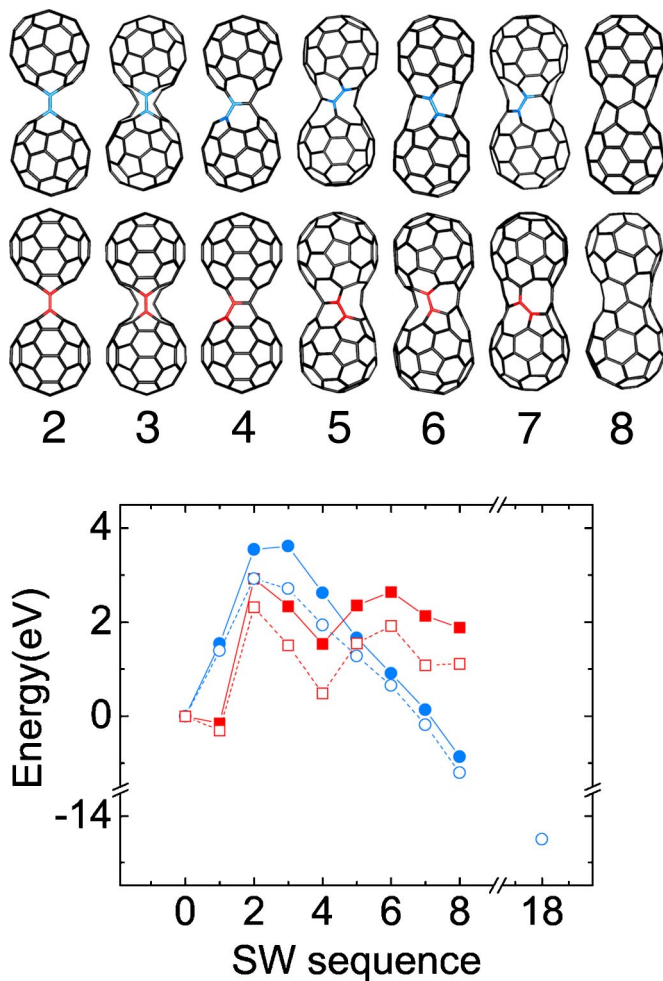


FIG. 1. (Color online) Two sequences (top) represent the two possible SW paths in which the C_{60} -pairs coalesce into the sections of (5,5) tubes. For each path seven (2–8) intermediate structures are shown; the colored bonds are those to be rotated. Numbers 0 and 1 are the separate and the dimerized buckyballs. The lower plots show the energy evolution for the corresponding $\mathbf{P}(\mathbf{P}$ and $\mathbf{5}(\mathbf{5}'$ paths, in squares and circles respectively. Hollow and solid indicate tight-binding Ref. 15 and *ab initio* density functional theory calculations [B3LYP with 3-21G basis set in Gaussian package (Ref. 16)]. Red and blue colors mark the $\mathbf{P}(\mathbf{P}$ and $\mathbf{5}(\mathbf{5}'$ paths.

the C_{60} 's is identical to the (5,5) SWNT caps, with a half of each C_{60} involved in coalescence. That is why the $\mathbf{5}(\mathbf{5}'$ path consists of only 16 SW steps, six steps shorter than the path $\mathbf{P}(\mathbf{P}$, which requires global reorientation of the whole C_{60} structure.

Figure 1 shows that the $\mathbf{P}(\mathbf{P}$ path has a somewhat lower barrier than the $\mathbf{5}(\mathbf{5}'$, and the standard dimerization should naturally be assumed to be the initial step of coalescence. However, relating the $\mathbf{P}(\mathbf{P}$ path to multiple C_{60} fusion inside a thicker tube¹⁴ runs into serious difficulty: C_{60} cannot approach the cap of a (5,5) tube in such an orientation; if one assumes that the coalescence starts from an already polymerized chain of C_{60} 's, then to accommodate the reorientations during the fusion process is impossible. In contrast, the $\mathbf{5}(\mathbf{5}'$ path does not require reorientation, is directly repeat-

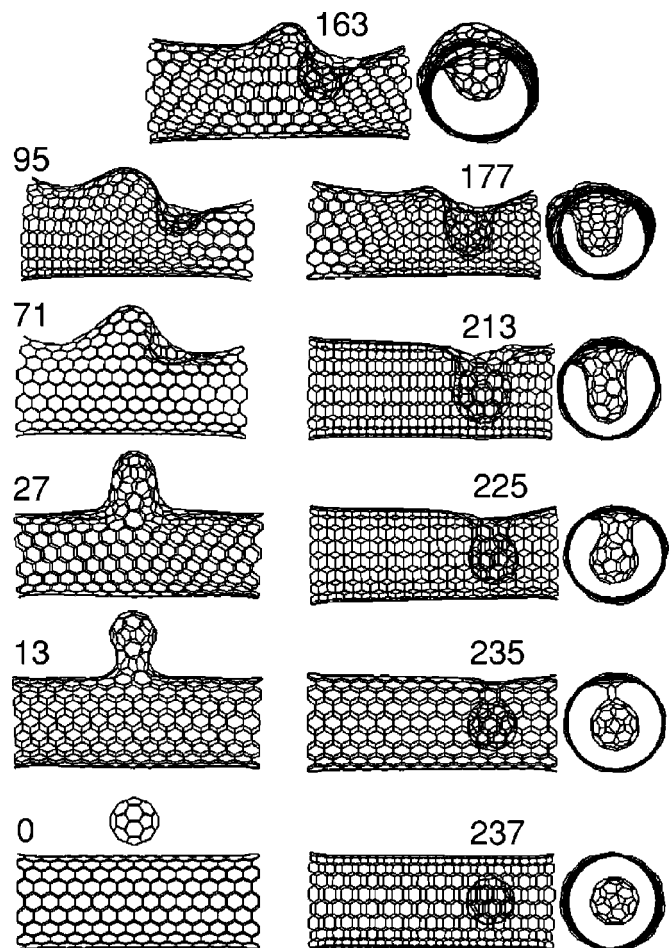


FIG. 2. A sequence of individual SW rotations (following initial covalent linking) has been identified for an extensive gradual morphing, where a buckyball completely penetrates the wall of a nanotube. Morphological change resembles the process of endocytosis in cellular biology (Ref. 17). Details are described in the text, but overall result of C_{60} encapsulation leads to a peapod structure. The rightmost column shows the axial views of the tube.

able in a series of C_{60} , and has a good transferability to nanotubes.

Recently, an action-derived molecular dynamics simulation of C_{60} coalescence⁵ identified the later ten SW rotations of the $\mathbf{5}(\mathbf{5}'$ path. Instead of polymerization and six bond rotations leading to the primary (5,0) neck structure, a gradual opening of the two apex pentagons is observed, due to the rigid initial orientation in the simulation. This small opening in the initial stage might be feasible, especially when the process is far from equilibrium. One more distinct possibility is a hexagon-to-hexagon $\mathbf{6}(\mathbf{6}'$ docking of buckyballs.⁵ The path found had noticeably higher activation barrier than in the $\mathbf{5}(\mathbf{5}'$ case. Neither $\mathbf{P}(\mathbf{P}$ nor $\mathbf{6}(\mathbf{6}'$ paths are possible for the coalescence of icosahedral cap pairs, with pentagons at the cap apices.

As mentioned above, although the initial steps specifically depend on the mutual docking orientation of the cages, a continuous SW path can usually be found, generally guided by a macroscopic scenario of the emerging and widening neck. The question one may ask is how versatile are these

paths? Motivated by the phenomenon of peapod formation¹⁴ and the morphological changes known in cellular biology as processes of endocytosis,¹⁷ we have attempted to identify a topological path for a penetration of C_{60} into an intact nanotube. Surprisingly, such morphing turns out to be topologically possible, as Fig. 2 demonstrates.

Figure 2 shows only the key snapshots¹⁸ of the above process. The initial point is a buckyball outside a (10,10) tube, denoted as no. 0 (step 0). The initial steps are the same as in C_{60} dimerization, except that the tube bond in the four-member ring is a circumferentially aligned one, more strained and hence easier to break. In the second step, two bonds in the four-member ring, other than those formed in polymerization, break to restore a shell structure to the whole system so that only SW rotations follow. In the neck structure at step no. 13, eight heptagons are found around the neck while eight other pentagons are left on the cap, and from this step no polygons larger than a heptagon are needed. At no. 27, the neck is larger than the cap and a hump is gradually formed from the original C_{60} . The total energy gets lower as the mount spreads. Therefore, energy consideration would favor a lower hump, as flat as possible. We found through trials that less than 100 steps would produce a mount with the lowest energy, containing only two pentagons on the top and two heptagons at the base. So far, the SW path was derived following essentially the same rules as in Ref. 4.

However, at this point, the energy begins to increase, in qualitative agreement with the visual curvature change: while the hump's exterior smoothens, a concavity formation begins, first with two pentagons and several surrounding heptagons, no. 71. These two pentagons are positioned in the same way as in C_{60} , serving as a nucleus of the aimed interior C_{60} . Further, the atoms are transported from the exterior hump to the bottom of the deepening concavity (from a mass-transport point of view), and more pentagons are created in the concavity (following the topology requirements for the emerging C_{60} structure). This is shown in steps no. 71 through no. 177. A "bud" capped by a semisphere of C_{60} in no. 213 introduces a large strain, which is then released through necking-off, no. 225. The following is approximately the reverse of the initial steps no. 0–13, ultimately leading to a separate, nested buckyball after two non-SW instances of rebonding and bond breaking occur after no. 235.

Figure 3 shows the energy changes along the complete SW sequence of 238 metastable structures (local minima). For faster calculations, Tersoff-Brenner potential¹⁹ is used and the ends of the (10,10) tube are free. No van der Waals (vdW) interaction is included. With vdW interaction considered, estimates show that the final state energy should be ~ 2.7 eV lower than the initial state because of the stronger vdW attraction for the interior C_{60} ,²⁰ and the barrier should also be lowered by $\sim 1-2$ eV. The overall barrier of 12 eV is very high from a thermal point of view (approximately 0.1 eV per atom involved in the transformation), so the process

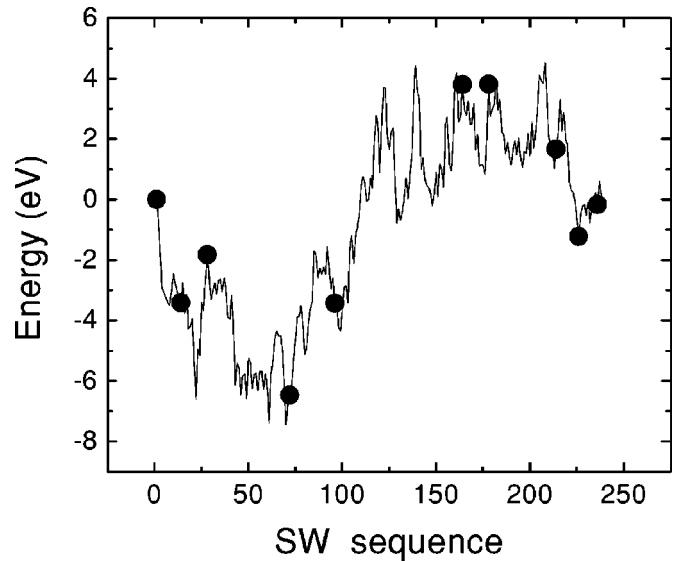


FIG. 3. Energies of 238 intermediate metastable structures (computed with multibody Tersoff-Brenner potential) for the process of "peapod endocytosis." Highlighted are the energies corresponding to the subset shown in Fig. 2, where the topmost structure has the highest energy due to the high strain involved.

may not be physically feasible although the topological path is clearly found. However, this energy corresponds to about 5% of mechanical strain, and therefore can be significantly reduced by bending deformations, from a random disturbance in the turbulent environment or applied deliberately, if possible. Another facilitating factor can be defects, especially vacancies in the wall. In an extreme case wall penetration can be aided by a large hole of opening, where the C_{60} adsorbed nearby can fall through (driven by reduction in the vdW potential mentioned above), as recently discussed in detail.²¹

In summary, through topological analysis based on Stone-Wales bond rotations, we have identified and compared possible reaction paths corresponding to coalescence of two C_{60} or cap-cap tube coalescence. Although there is yet no direct experimental identification of the paths at the atomic level, the energetically favorable and topologically transferable SW sequence seems to be highly plausible for the C_{60} coalescence.²³ We have also demonstrated the SW sequence for a C_{60} penetration through the wall of a carbon nanotube. Its energy barrier is very high, but might be reduced by mechanical bending or other concurrent deformation or defects in the wall. Although unlikely feasible from the energy barrier point of view, perfect wall permeation shows topological versatility of SW paths in fullerene shape transformations.

We would like to thank David Tomanek for a useful reference and discussion at the APS March meeting. This work was supported by the National Science Foundation, Grant No. EEC-0118007 (CBEN).

- *Corresponding author. Electronic address: biy@rice.edu
- ¹A.J. Stone and D.J. Wales, *Chem. Phys. Lett.* **128**, 501 (1986); S.J. Austin, P.W. Fowler, D.E. Manolopoulos, and F. Zerbetto, *ibid.* **235**, 146 (1995); D.J. Wales, M.A. Miller, and T.R. Walsh, *Nature (London)* **394**, 758 (1998).
- ²H. Ueno, S. Osawa, E. Osawa, and K. Takeuchi, *Fullerene Sci. Technol.* **6**, 319 (1998).
- ³Y. Zhao, B.I. Yakobson, and R.E. Smalley, *Phys. Rev. Lett.* **88**, 185501 (2002).
- ⁴Y. Zhao, R.E. Smalley, and B.I. Yakobson, *Phys. Rev. B* **66**, 195409 (2002).
- ⁵Y.-H. Kim, I.-H. Lee, K.J. Chang, and S. Lee, *Phys. Rev. Lett.* **90**, 065501 (2003).
- ⁶B.I. Yakobson, *Appl. Phys. Lett.* **72**, 918 (1998); M. Buongiorno Nardelli, B.I. Yakobson, and J. Bernholc, *Phys. Rev. Lett.* **81**, 4656 (1998).
- ⁷See discussion in T. Dumitrica, T. Belytschko, and B.I. Yakobson, *J. Chem. Phys.* **118**, 9485 (2003).
- ⁸S. Wang, and P.R. Buseck, *Chem. Phys. Lett.* **182**, 1 (1991); P. Nikolaev, A. Thess, A.G. Rinzler, D.T. Colbert and R.E. Smalley, *ibid.* **266**, 422 (1997); M. Terrones, H. Terrones, F. Banhart, J.-C. Charlier, and P.M. Ajayan, *Science* **288**, 1226 (2000); M. Terrones, F. Banhart, N. Grobert, J.-C. Charlier, H. Terrones, and P.M. Ajayan, *Phys. Rev. Lett.* **89**, 075505 (2002).
- ⁹*Fullerene Polymers and Fullerene Polymer Composites*, edited by P.C. Eklund and A.M. Rao (Springer, Berlin, 2000).
- ¹⁰D.L. Strout, R.L. Murry, C. Xu, W.C. Eckhoff, G.K. Odom, and G.E. Scuseria, *Chem. Phys. Lett.* **214**, 576 (1993).
- ¹¹H. Terrones and A.L. Mackay, *Chem. Phys. Lett.* **207**, 45 (1993).
- ¹²*Handbook of Nanoscience, Engineering, and Technology*, edited by W.A. Goddard III, D.W. Brenner, S.E. Lyshevski, and G.J. Iafrate (CRC Press, Boca Raton, 2003).
- ¹³The *nucleation* barrier is determined by the highest-energy metastable intermediate structure, and does not include the *activation* barrier of transition state, which by itself is high (5–9 eV, depending on degree of local strain in the lattice) for each SW step, since it involves rearrangement of two carbon bonds. However, this activation barrier can be in principle reduced by catalyst (Ref. 22) or overcome by light or electron-beam radiation (Ref. 8). In contrast, the energy points discussed here correspond to chemically inert structures and cannot be reduced by similar factors.
- ¹⁴B.W. Smith and D.E. Luzzi, *Chem. Phys. Lett.* **321**, 169 (2000); J. Sloan *et al.*, *ibid.* **316**, 191 (2000).
- ¹⁵D. Porezag, T. Frauenheim, T. Kohler, G. Seifert, and R. Kaschner, *Phys. Rev. B* **51**, 12 947 (1995); see also C.M. Goringe, D.R. Bowler, and E. Hernandez, *Rep. Prog. Phys.* **60**, 1447 (1997).
- ¹⁶M.J. Frisch, G.W. Trucks, H.B. Schlegel, G.E. Scuseria *et al.*, GAUSSIAN 98, Revision A.6 (Gaussian Inc., Pittsburgh, 1998). B3LYP stands for Becke's three-parameter hybrid method using Lee-Yang-Parr correlation functional.
- ¹⁷B. Alberts, D. Bray, J. Lewis, M. Raff, K. Roberts, and J.D. Watson, *Molecular Biology of the Cell* (Garland, New York, 1994).
- ¹⁸See EPAPS Document No. E-PRBMDO-68-016343 for full sequence corresponding to Fig. 2 animated as MPG files. A direct link to this document may be found in the online article's HTML reference section. The document also may be reached via the EPAPS homepage (<http://www.aip.org/pubservs/epaps.html>) or from <ftp.aip.org> in the directory /epaps/. See the EPAPS homepage for more information.
- ¹⁹J. Tersoff, *Phys. Rev. B* **37**, 6991 (1988); D.W. Brenner, *ibid.* **42**, 9458 (1990).
- ²⁰L.A. Girifalco, M. Hodak, and R.S. Lee, *Phys. Rev. B* **62**, 13 104 (2000).
- ²¹S. Berber, Y.-K. Kwon, and D. Tomanek, *Phys. Rev. Lett.* **88**, 185502 (2002).
- ²²B.R. Eggen, M.I. Heggie, G. Jungnickel, C.D. Latham, R. Jones, and P.R. Briddon, *Science* **272**, 87 (1996); P. Jensen, J. Gale, and X. Blase, *Phys. Rev. B* **66**, 193403 (2002).
- ²³See recent report, E. Hernandez, V. Meunier, B.W. Smith, R. Rurali, H. Terrones, M. Buongiorno Nardelli, M. Terrones, D.E. Luzzi, and J.C. Charlier, *Nano Lett.* **3**, 1037 (2003).